

# Effect of Co-addition of Sn, Traces of RE and Ca on the Mechanical and Micro Structural Properties of As-cast AZ80 Alloy

Madhusudhanprasad MANCHALA \*, Ramachandra Raju VEGESNA

Department of Mechanical Engineering, JNT University College of Engineering Kakinada (A), Kakinada, Andhra Pradesh, 533003, India

<http://doi.org/10.5755/j02.ms.35474>

Received 3 November 2023; accepted 2 April 2024

In this study, the effect of co-addition of tin (0, 6 and 9 wt.%), cerium (0, 0.3 and 0.6 wt.%), gadolinium (0, 0.6 and 0.9 wt.%) and calcium (0, 0.6 and 0.9 wt.%) on the mechanical and microstructural properties of AZ80 magnesium alloy is investigated. The results indicate that the mechanical properties are improved for all the as-cast alloys when compared to base alloy except for one alloy which is due to the presence of Mg-Sn-Ca phase in high volume fraction. Also, it is found that the existence of Al<sub>2</sub>Ca, Mg<sub>2</sub>Ca, Al<sub>2</sub>RE, MgSnRE and Mg<sub>2</sub>Sn phases have a significant impact on the mechanical and microstructural characteristics of the as-cast AZ80 alloys. It is observed that without the addition of Sn content, the best room temperature tensile properties are obtained for the alloy containing 1.5 wt.% of RE and 0.9 wt.% of Ca. With the addition of Sn, it is found that the best room temperature tensile properties are obtained for the alloy containing 6 wt.% of Sn, 0.9 wt.% of RE and 0.5 wt.% of Ca.

*Key words:* magnesium alloy, rare earth metal, casting, microstructure, mechanical properties.

## 1. INTRODUCTION

Due to their lower density, excellent damping capacity, and widespread availability, magnesium (Mg) alloys are being used [1–3] in areas that are experiencing significant growth, such as the automotive and aerospace industries. Generally, for low-temperature applications, Mg cast alloys like Mg-(6 to 9 wt.%) aluminum (Al) alloys are frequently used. Furthermore, these Mg-Al alloys can be used for high temperature applications when they are alloyed with proper alloying elements. The results from several reports [4–7] demonstrate how the inclusion of Tin (Sn) improved the mechanical properties and corrosion rates of the Al series of magnesium alloys. However, this improvement is limited due to the formation of the Mg<sub>17</sub>Al<sub>12</sub> phase. Due to the ability to enhance creep resistance and tensile strength, calcium (Ca) is generally added to Mg alloys [8]. Yanfu Chai, et al studied [9] the properties of Mg-Sn-Zn alloy with the minor addition of Ca content and found that the mechanical properties are improved while the Mg<sub>2</sub>Sn phase transforms into Ca-Mg-Sn and Mg<sub>2</sub>Ca phases. Also, the combination of Sn and Ca in Mg-Zn-Al alloy [10] is found to enhance the mechanical properties. Recently, investigations have been carried out [11] on the addition of rare earth (RE) elements in Mg alloys to improve the mechanical properties and refine microstructure. It is reported that [12–14] alloying of either single RE or a combination of REs to the AZ series alloy led to the grain refinement and Al<sub>2</sub>RE phase formation which in turn improved the corrosion resistance and mechanical properties. Jiang, et al pointed out [14] that when Neodymium (Nd) and Gadolinium (Gd) are added to AZ80 alloy in small quantities, an effective modification in the microstructure is found to result in the growth of Al-RE-Mn,

Al<sub>11</sub>RE<sub>3</sub>, and Al<sub>2</sub>RE phase. Yang, et al studied [15] the variation of microstructure and age hardening behaviour in Mg-6Zn-1Mn-4Sn alloy with minor Gd additions and found the finely grown Mg<sub>7</sub>Zn<sub>3</sub>, Mg<sub>2</sub>Sn, and Mg-Sn-Gd phases. They pointed out that due to the refinement of grains, higher density precipitation occurs, and the retainment of dislocations resulted in the increase of strength in 0.2 wt.% Gd alloy.

Cerium (Ce) is one of the abundantly available RE which can significantly affect the properties of Mg alloys when added in small amounts. It is reported [16] that 0.2 wt.% Ce in Pure Mg followed by its extrusion resulted for improved ductility. When Ce is added up to 1.5 wt.% in ZK60 alloy, it is found to result [17] in the reduction of average grain size and improvement in ultimate tensile strength but at the cost of ductility.

Furthermore, Chaojie Che, et. al [18] investigated the effect of the co-addition of Si, Ca & RE on AZ91 alloy and found that these alloying elements influenced the microstructure and mechanical properties. Similarly, other studies [19–21] also reported that trace addition of alloying elements leads to the improvement of properties and change of microstructure.

Although from the above studies, it is evident that combined addition or trace additions of alloying elements can improve the mechanical properties in certain Mg alloys, the combined effect of alloying elements on Mg-8Al alloy is rarely reported. In the present work, the influence of the co-addition of Sn, REs and Ca on Mg-8Al alloy (B) is investigated through the casting route.

## 2. EXPERIMENTAL DETAILS

To study the combined influence of Sn (0, 6 and 9 wt.%) content and traces of Ce (0, 0.3 and 0.6 wt.%),

\*Corresponding author. +91-9966915354.

E-mail: [msprasad@jntucek.ac.in](mailto:msprasad@jntucek.ac.in) (M. Manchala)

Gd(0, 0.6 and 0.9 wt.%) and Ca(0, 0.5 and 0.9 wt.%) on the properties of AZ80 alloy, nine alloys are chosen (based on the Design of experiments through Taguchi approach) and cast. The chemical compositions of the casted alloy(s) are listed in Table 1. Commercially available pure metals like Mg, Al, Zn, Si, Sn, Gd, and Ce are used. Manganese (Mn) and calcium (Ca) are added as Mg-15%Mn and Mg-10%Ca master alloys. A temperature refractory crucible with pure magnesium ingots is placed inside an INDFURR Induction furnace and heated initially up to 850 °C in the presence of high purity SF<sub>6</sub> gas (99.9 %). All the necessary alloying elements are added to the magnesium melt. The alloy is maintained at a temperature of 720 °C for around 40 minutes. Then, the molten metal is transferred to a preheated (300 °C–400 °C) alloy steel mould of volume 25 cm × 20 cm × 3 cm. An INDFURR Oven is used for preheating the steel mould. Fig. 1 shows the experimental setup, crucible, steel mould, oven, and as-cast samples.

Casted samples are tested according to ASTM B557-02a standard using an FIE-UTE Universal Testing Machine to find the ultimate tensile strength (UTS), yield strength (YS) and percentage elongation (%E). The hardness test is conducted using a FIE- B3000 Brinell hardness machine

**Table 1.** Chemical composition (wt.%) of as-cast AZ80 (B) alloys

| Alloy | Al  | Zn  | Si  | Mn   | Sn | Ce  | Gd  | Ca  | Mg   |
|-------|-----|-----|-----|------|----|-----|-----|-----|------|
| B1111 | 8.5 | 0.5 | 0.1 | 0.12 | –  | –   | –   | –   | Bal. |
| B1222 | 8.5 | 0.5 | 0.1 | 0.12 | –  | 0.3 | 0.6 | 0.5 | Bal. |
| B1333 | 8.5 | 0.5 | 0.1 | 0.12 | –  | 0.6 | 0.9 | 0.9 | Bal. |
| B2213 | 8.5 | 0.5 | 0.1 | 0.12 | 6  | 0.3 | –   | 0.9 | Bal. |
| B2321 | 8.5 | 0.5 | 0.1 | 0.12 | 6  | 0.6 | 0.6 | –   | Bal. |
| B2132 | 8.5 | 0.5 | 0.1 | 0.12 | 6  | –   | 0.9 | 0.5 | Bal. |
| B3312 | 8.5 | 0.5 | 0.1 | 0.12 | 9  | 0.6 | –   | 0.5 | Bal. |
| B3123 | 8.5 | 0.5 | 0.1 | 0.12 | 9  | –   | 0.6 | 0.9 | Bal. |
| B3231 | 8.5 | 0.5 | 0.1 | 0.12 | 9  | 0.3 | 0.9 | –   | Bal. |

with a tungsten (W) indenter. Samples are tested under an optical microscope (OM) after grit by 180, 240, 320, 400, 600, 800, 1000, 1500, and 2000 grits followed by polishing with Al<sub>2</sub>O<sub>3</sub> powder and etched with acetic acid- picric acid- ethanol solution. Scanning electron microscope (SEM) and Energy dispersive spectroscopy (EDS) are used to observe the microstructure in detail. X-ray diffraction (XRD) is used to identify the phase constituents of the alloys.

### 3. RESULTS AND DISCUSSION

In the present work, Sn, Gd, Ce and Ca metals are added to Mg-8Al (B) based magnesium alloy through the casting route. The impact of these elements on the mechanical and micro structural properties of as-casted Mg-8Al based alloys is presented here.

#### 3.1. Microstructural study

XRD patterns exhibited by casted alloys are illustrated in Fig. 2. The base alloy B1111 is found to consist of a primary Mg phase and a secondary Mg<sub>17</sub>Al<sub>12</sub> phase. In general [4, 8, 15, 23], greater electronegativity (EN) between elements will lead to the easier formation of intermetallic compounds during solidification.

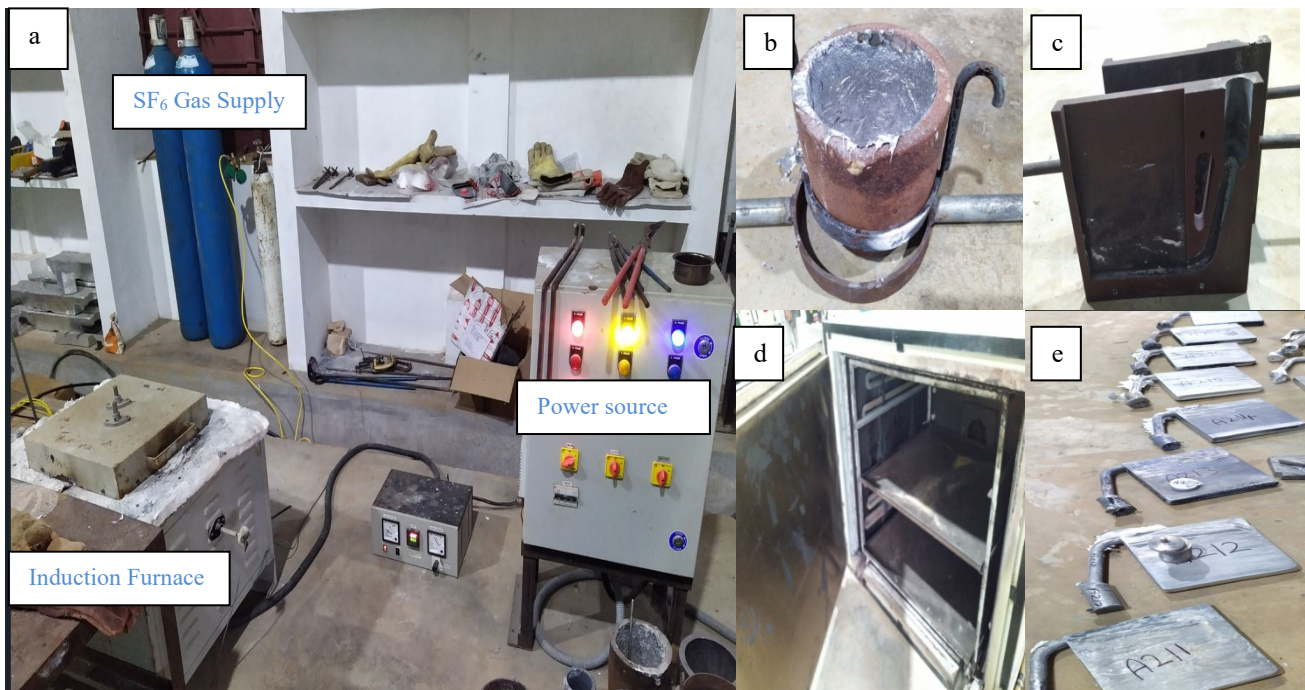


**Fig. 1.** a – experimental setup; b – refractory crucible; c – steel mould; d – oven; e – as-cast samples (Photo courtesy @ MatRICS, Nagercoil, India)

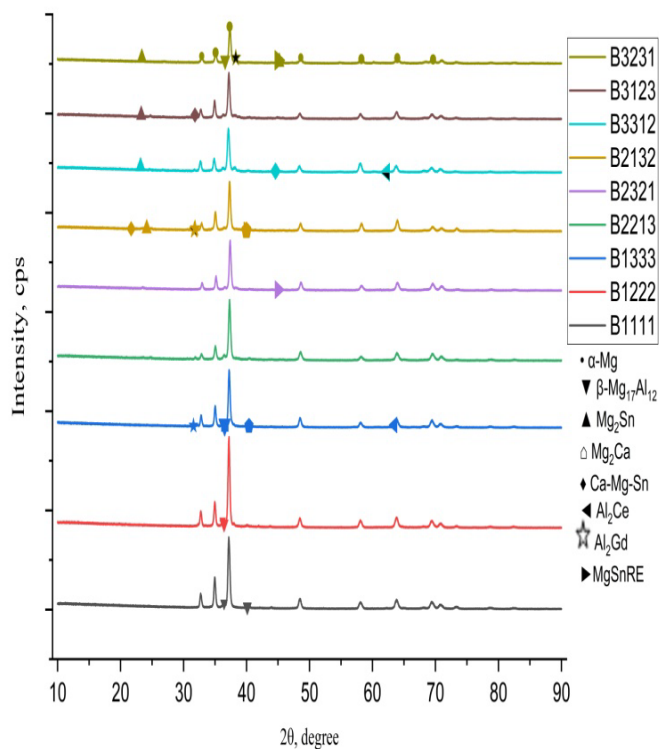


**Fig. 2.** XRD patterns of casted AZ80 alloys

The electro negativity difference between Mg-Al, Mg-Sn, Mg-Si, Al-Ce, Al-Gd, and Al-Ca are 0.30, 0.65, 0.59, 0.45, 0.41 and 0.61 respectively. As reported by B. Pourbahari, et. al [22], the  $Al_2RE$  phase is observed to be formed at the expense of the secondary  $Mg_{17}Al_{12}$  phase. It is also observed that when Sn is added to Mg-8Al alloy, the formation of  $Mg_2Sn$  (with EN of 0.65) is predominant when compared to Al-Sn (with EN of 0.35). Furthermore, for alloys with RE content ( $> 0.3$  wt.%),  $Al_2RE$  is likely to be formed and for the alloys with Ca addition,  $Al_2Ca$  formation is easier when compared to  $Mg_2Ca$  based on EN. For B2213, B3312 and B3123 alloys, the Mg-Sn-Ca phase is observed to be formed. The above observations can be confirmed from XRD peaks and SEM-EDS analysis.

Optical microscopic images of cast alloys are presented in Fig. 3. In B1111 alloy, secondary  $Mg_{17}Al_{12}$  phase is found to be formed which is verified from the XRD pattern. This phase is found to be distributed along the boundaries of grains and into the spaces between dendrites. For B1222 alloy, coarse grains are observed. The formation of a secondary  $Mg_{17}Al_{12}$  phase is observed for all the casted alloys. In B1333 alloy, fine grains are formed when compared to B1222 alloy and fine precipitates (small-block shaped) are found [14] to get dispersed along the grain boundaries and within the grains. These fine precipitates can be attributed to  $Al_2RE$  and  $Mg_2(Si, Ca)$  phases observed from XRD peaks and SEM-EDS analysis. For B2213, B3312 and B3123 alloys more coarsening trend of grains is observed. In B2321, and B2132 alloys, the precipitate formation is more especially in B2132 alloy which is attributed to the presence of small-block shaped  $Al_2RE$  and  $Mg_2Sn$  phases. In B2213 and B3123 alloys, a needle like Mg-Sn-Ca phase is found [23] to be formed. This formation of Mg-Sn-Ca will reduce the amount of  $Mg_2Sn$  which can

be ascribed to earlier nucleation of Mg-Sn-Ca phase prior to  $Mg_2Sn$  according to EN value [15]. For B3231 alloy, lesser coarsening of grains with small-block shaped  $Al_2RE$  and  $Mg_2Sn$  phases are seen to be dispersed along the grain borders and within the grains.

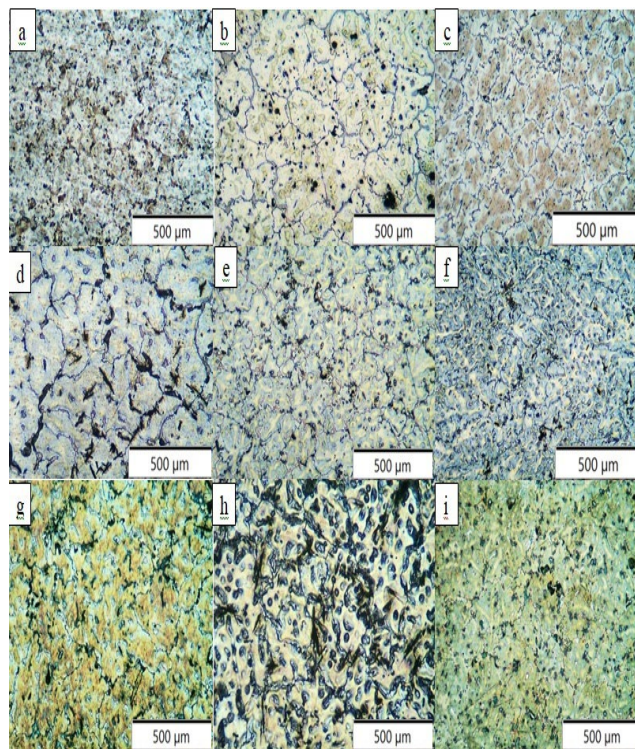


**Fig. 3.** Optical microscopic images: a–B1111; b–B1222; c–B1333; d–B2213; e–B2321; f–B2132; g–B3312; h–B3123; i–B3231 alloys

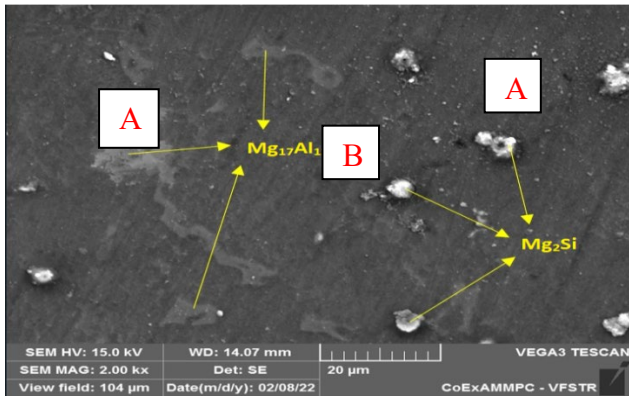
### 3.2. SEM analysis

The SEM image for B1111 as cast alloy is given in Fig. 4 a and EDAX spectrum is shown in Fig. 4 b. The EDAX result for Fig. 4 a is listed in Table 2. The secondary  $Mg_{17}Al_{12}$  phase is observed to be dispersed in the primary Mg phase. The small precipitates are found to be formed as  $Mg_2Si$  particles. However, the diffraction peak for the same is not visible in the XRD pattern. This similar trend reported elsewhere [14] is due to the grown phase's low volume proportion as compared to primary or secondary phases.

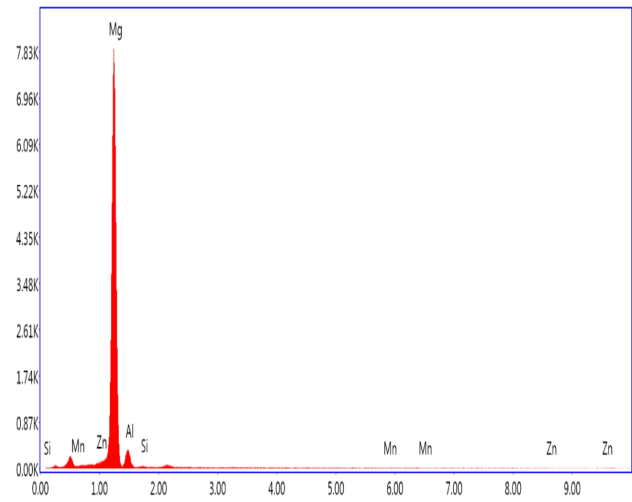
The SEM image for as cast B2132 alloy is displayed in Fig. 5 a and EDAX spectrum is shown in Fig. 5 b. The EDAX result for Fig. 5 a is listed in Table 3. The secondary  $Mg_{17}Al_{12}$  phase is observed to be dispersed in the primary phase in this alloy. The growth for  $Mg_2Sn$ ,  $Al_2Gd$  and  $Mg_2Ca$  phases is confirmed by the elemental mapping and the XRD peaks. The volume fraction of  $Mg_2Sn$  and  $Al_2Gd$  is found to be more than  $Mg_2Ca$  since the volume proportion of Ca is less. This observation is confirmed by SEM-EDS analysis and the XRD peaks.

The SEM image for as cast B1333 alloy is illustrated in Fig. 6 a and EDAX spectrum is shown in Fig. 6 b. The EDAX result for Fig. 6 a is listed in Table 4. In this alloy,  $Al_2RE$ ,  $Mg_2(Si, Ca)$  phases are observed to exist in precipitate form. It is also observed that the volume proportion of the  $Al_2Ca$  phase is more prevalent than that of the  $Al_2RE$  and  $Mg_2(Si, Ca)$  phases.



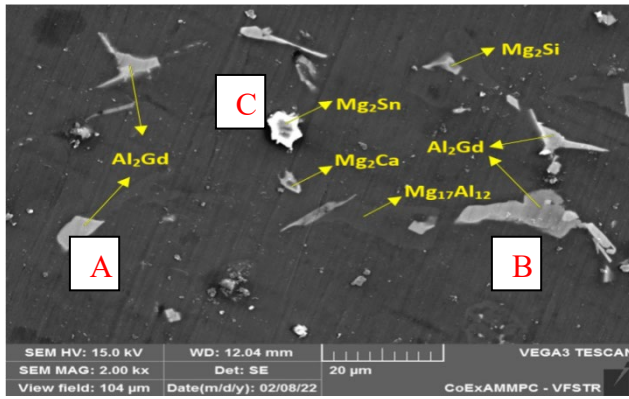


a

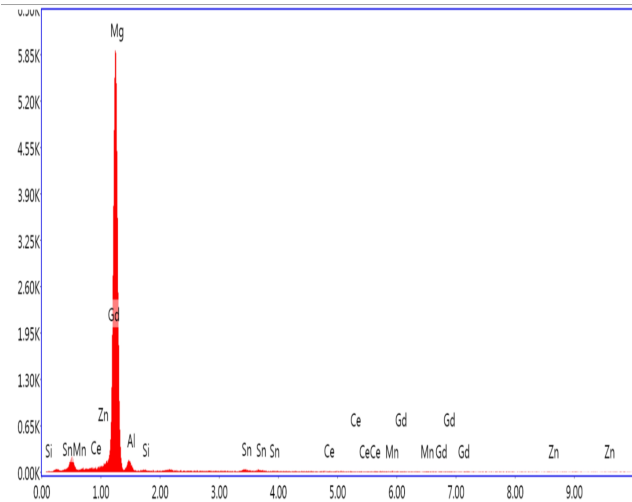


b

Fig. 4. a – SEM image; b – EDAX spectrum of B1111 alloy



a



b

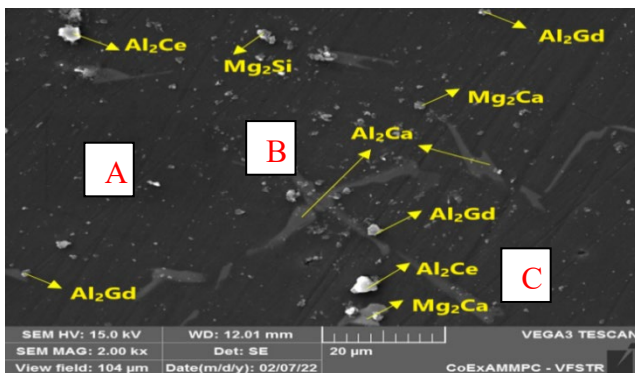
Fig. 5. a – SEM image; b – EDAX Spectrum of B2132 Alloy

Table 2. EDAX results of Fig. 4 a

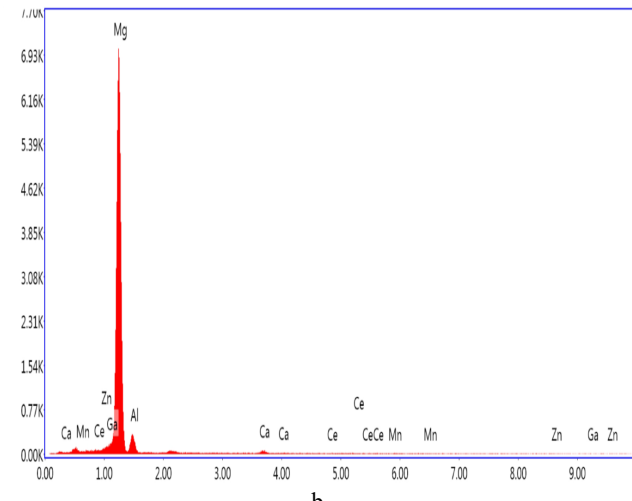
| Region (R) | Mass fraction percentages |       |       |      |      |
|------------|---------------------------|-------|-------|------|------|
|            | Mg                        | Al    | Si    | Mn   | Zn   |
| A          | 70.73                     | 25.39 | 0.71  | 0.90 | 2.27 |
| B          | 74.56                     | 3.42  | 20.76 | 0.26 | 1.00 |

Table 3. EDAX results of Fig. 5 a

| R | Mass fraction percentages |     |     |     |     |      |      |     |
|---|---------------------------|-----|-----|-----|-----|------|------|-----|
|   | Mg                        | Al  | Si  | Mn  | Zn  | Sn   | Ca   | Gd  |
| A | 82.2                      | 8.6 | 0.1 | 0.6 | 2.0 | 4.4  | 0.9  | 1.2 |
| B | 79.2                      | 2.9 | 0.3 | 0.4 | 0.6 | 1.0  | 15.1 | 0.5 |
| C | 68.2                      | 1.0 | 0.4 | 0.3 | 0.5 | 25.6 | 3.8  | 0.2 |

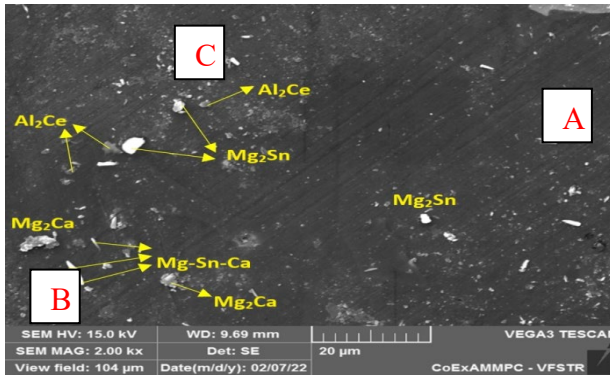


a

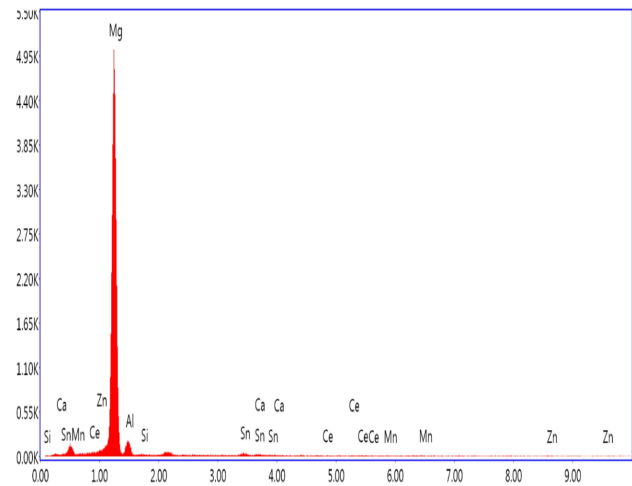


b

Fig. 6. a – SEM image; b – EDAX Spectrum of B1333 Alloy



a



b

**Fig. 7.** a – SEM image; b – EDAX Spectrum of B2213 Alloy

**Table 4.** EDAX results of Fig. 6 a

| R | Mass fraction percentages |      |      |      |     |      |     |
|---|---------------------------|------|------|------|-----|------|-----|
|   | Mg                        | Al   | Mn   | Zn   | Si  | Ca   | Ce  |
| A | 84.7                      | 9.1  | 0.49 | 2.72 | 0.4 | 1.8  | 0.9 |
| B | 11.0                      | 72.1 | 0.4  | 0.5  | 0.2 | 15.1 | 0.7 |
| C | 73.2                      | 2.9  | 0.3  | 0.4  | 0.6 | 21.6 | 1.0 |

**Table 5.** EDAX results of Fig. 7 a

| R | Mass fraction percentages |      |     |     |      |      |      |      |
|---|---------------------------|------|-----|-----|------|------|------|------|
|   | Mg                        | Al   | Si  | Mn  | Zn   | Sn   | Ca   | Ce   |
| A | 83.3                      | 7.52 | 0.4 | 0.5 | 4.55 | 2.87 | 0.15 | 0.71 |
| B | 22.4                      | 1.5  | 0.1 | 0.6 | 0.9  | 62.0 | 11.6 | 0.9  |
| C | 6.4                       | 70.4 | 0.0 | 0.1 | 0.5  | 1.5  | 0.9  | 20.2 |

The precipitates are observed to be randomly dispersed in both of the primary Mg and secondary  $Mg_{17}Al_{12}$  phases.

The SEM image of the B2213 alloy is presented in Fig. 7 a and EDAX spectrum is shown in Fig. 7 b. The EDAX result for Fig. 7 a is listed in Table 5. In this alloy,  $Mg_2$  (Sn, Ca) phase and  $Al_2Ce$  phase are found to grow in the form of precipitates. From the OM image of B2213 alloy, it is evident that needle like Mg-Sn-Ca phase is grown as verified from XRD peaks and SEM-EDS image.

### 3.3. Mechanical properties

The estimated properties like UTS, YS, %E, Brinell hardness number (BHN) of the cast alloys are presented in Table 6, while their trends are represented in Fig. 8. Also, the percentage enhancement of properties when compared to base alloy i.e., B1111 alloy are indicated in Table 6. The as-cast alloy B2132 is found to possess UTS of 208 MPa followed by B1333 with 204 MPa and B2321 with 193 MPa. Likewise, YS is found to be high for B3231 with 155 MPa followed by B2132 with 152 MPa and B2321 with 151 MPa. The percentage elongation is high for B2132 and B1333 at 9 % followed by B2321 with 7.5 %. The hardness

is found to be high for B3312 and B3231 with 65 BHN followed by B3123 with 63 BHN. For B2132 alloy, the observed enhanced mechanical properties are attributed to the decrease in volume fraction of  $Mg_{17}Al_{12}$  phase due to the prior formation of thermally stable, high melting point temperature  $Mg_2Sn$ ,  $Al_2Gd$  phases and to the presence of low volume fraction of  $Mg_2(Si, Ca)$  phase. For B1333 alloy, the enhancement of properties is attributed to relatively finer grain size and the presence of precipitates which lead to dispersion strengthening as reported by Yang Zhao, et. al [15]. Also, the properties of Mg-8Al alloy are observed to be enhanced with the presence of the  $Al_2Ca$  phase and fine  $Al_2RE$  and  $Mg_2(Si, Ca)$  phases by preventing slippage dislocation motion which is well in agreement with previous studies [14, 21]. In B2213 alloy, coarse grains are found to exist with a relatively high-volume fraction of needle like Mg-Sn-Ca phase [23] as observed from OM image and SEM-EDS analysis. As such, they act as a potential site for the formation of micro cracks resulting in decreased properties. This decrement in the properties is also attributed to the presence of coarse precipitates dispersed in both the primary and secondary phases.

**Table 6.** Mechanical properties of as-cast AZ80 alloys and their percentage enhancement at ambient temperature

| Cast alloy | UTS, MPa | UTS percentage enhancement | YS, MPa | YS percentage enhancement | Percentage elongation, %E | Elongation percentage enhancement | BHN | Hardness percentage enhancement |
|------------|----------|----------------------------|---------|---------------------------|---------------------------|-----------------------------------|-----|---------------------------------|
| B1111      | 136      | –                          | 118     | –                         | 1.82                      | –                                 | 52  | –                               |
| B1222      | 152      | 11.8                       | 118     | 0                         | 6.7                       | 268                               | 56  | 7.7                             |
| B1333      | 204      | 50                         | 138     | 17                        | 9                         | 394                               | 53  | 2                               |
| B2213      | 127      | -6.6                       | 118     | 0                         | 4.2                       | 131                               | 58  | 11.5                            |
| B2321      | 193      | 42                         | 151     | 28                        | 7.5                       | 312                               | 49  | -6                              |
| B2132      | 208      | 53                         | 152     | 29                        | 9                         | 394                               | 60  | 15.4                            |
| B3312      | 151      | 11                         | 138     | 17                        | 3.2                       | 76                                | 65  | 25                              |
| B3123      | 153      | 12.5                       | 145     | 23                        | 6.6                       | 263                               | 63  | 21                              |
| B3231      | 168      | 23.5                       | 155     | 31                        | 5.3                       | 191                               | 65  | 25                              |

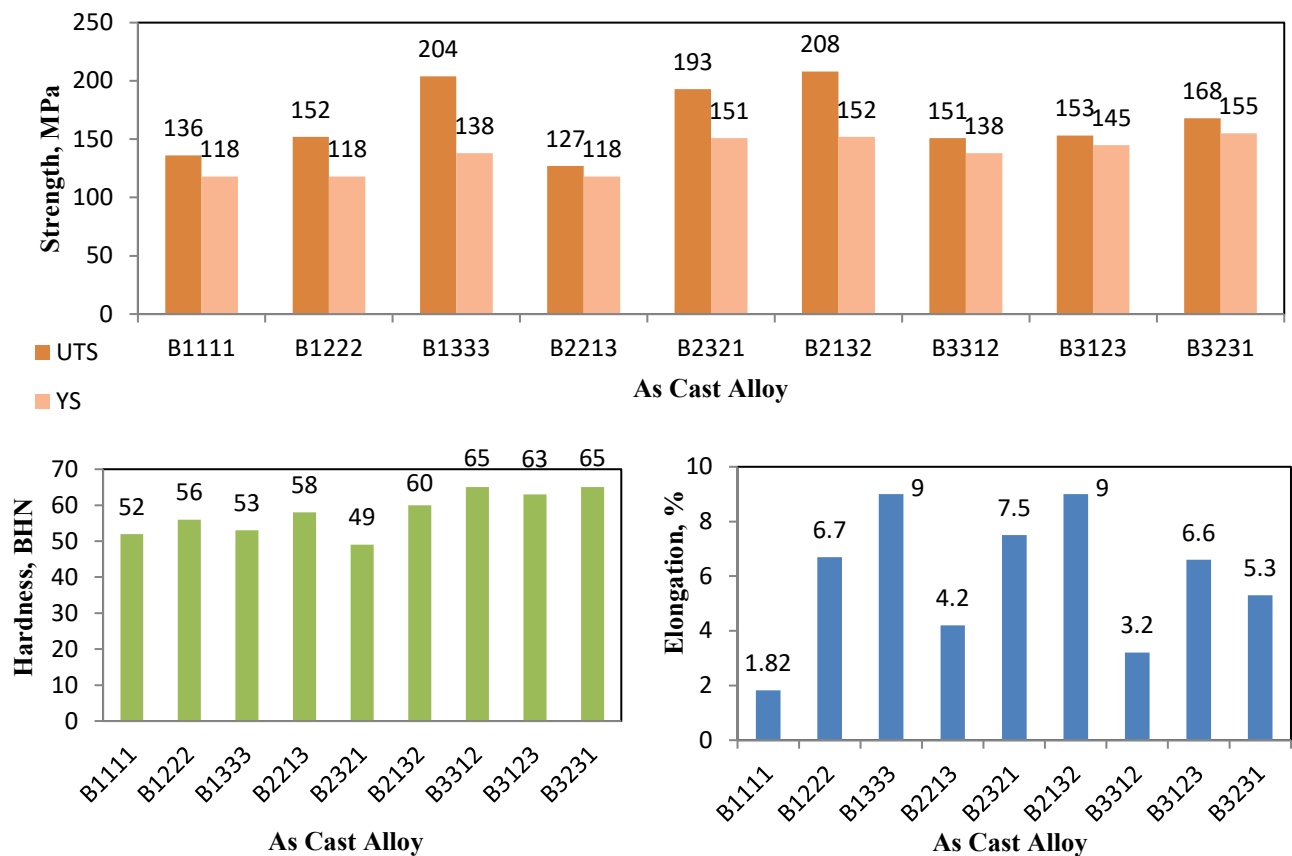


Fig. 8. Mechanical properties of the as-cast AZ80 alloys

Hence it can be concluded that B2132 and B1333 alloys which consist of thermally stable, high melting point temperature compounds in precipitate form inside the grains and along the grain boundaries can be used in light weight and moderate temperature applications that require 130 to 200 MPa strength at room temperature.

#### 4. CONCLUSIONS

To study the combined influence of Sn and trace elements of REs and Ca on the characteristics of as-cast AZ80 alloy, an experimental investigation using nine alloys is carried out through casting route. The important observations made are:

1. With the addition of Sn, the room temperature tensile strength of AZ80 alloy is enhanced due to the presence of fine precipitates of  $Mg_2Sn$  along the grain boundaries and within the grains except for B2213 alloy. For B2213 alloy the reduction of tensile strength is observed which is attributed to its coarse grain structure and high-volume fraction of the Mg-Sn-Ca phase. Furthermore, for the alloy containing 6 wt.% of Sn, 0.9 wt.% of RE and 0.5 wt.% of Ca, better enhancement of 53 % ultimate tensile strength is noted when compared to AZ80 alloy.
2. Without Sn addition, better properties are observed for the alloy containing 1.5 wt.% RE and 0.9 wt.% Ca i.e., an improvement of 50 % in tensile strength and 394 % in elongation is observed when compared to AZ80 alloy. This is due to the formation of thermally stable,

high melting point temperature  $Al_2(RE, Ca)$  precipitates.

3. Hence the co-addition of Sn, Ce, Gd & Ca in AZ80 alloy lead to refinement of microstructure in all as-cast alloys and changed the mechanical properties of AZ80 magnesium alloy significantly.

#### REFERENCES

1. Polmear, I. Light Alloys-From Traditional Alloys to Nano Crystals 4th ed. Oxford; Burlington, MA: Butterworth-Heinemann, 2005.
2. Luo, A., Pekguleryuz, M.O. Cast Magnesium Alloys for Elevated Temperature Applications *Journal of Materials Science* 29 1994: pp. 5259 – 5271.
3. Mordike, B.L., Ebert, T. Magnesium Properties–Applications–Potential *Journal of Materials Science and Engineering A* 302 2001: pp. 37 – 45.
4. Wang, B., Chen, X., Pan, F., Mao, J. Effects of Sn Addition on Microstructure and Mechanical Properties of Mg-Zn-Al Alloys *Journal of Progress in Natural Science: Materials International* 2017: pp. 695 – 702. <https://doi.org/10.1016/j.pnsc.2017.11.002>
5. Zengin, H., Turen, Y., Ahlatci, H., Sun, Y., Karaoglanli, A.C. Influence of Sn Addition on Microstructure and Corrosion Resistance of AS21 Magnesium Alloy *Transactions of Nonferrous Metals Society of China* 29 2019: pp. 1413 – 1423. [https://doi.org/10.1016/S1003-6326\(19\)65048-X](https://doi.org/10.1016/S1003-6326(19)65048-X)
6. Jiang, L., Zhang, D., Fan, X., Guo, F., Guangshan, H., Hansong, X., Pan, F. The Effect of Sn Addition on Aging

Behavior and Mechanical Properties of Wrought AZ80 Magnesium Alloy *Journal of Alloys and Compounds* 620 2015: pp. 368–375.  
<https://doi.org/10.1016/j.jallcom.2014.09.165>

7. **Dong, X., Fu, J., Wang, J., Yang, Y.** Microstructure and Tensile Properties of As-cast and As-aged Mg-6Al-4Zn Alloys with Sn Addition *Journal of Materials and Design* 51 2013: pp. 567–574.  
<https://doi.org/10.1016/j.matdes.2013.04.067>
8. **Yang, M.B., Cheng, L., Sheng, J., Pan, F.** Effect of Ca Addition on the As-cast Microstructure and Creep Properties of Mg-5Zn-5Sn Magnesium Alloy *Journal of Rare Metals* 28 2009: pp. 576–581.  
<https://doi.org/10.1007/s12598-009-0111-6>
9. **Chai, Y., Jiang, B., Song, J., Wang, Q., Gao, H., Liu, B., Huang, G., Zhang, D., Pan, F.** Improvement of Mechanical Properties and Reduction of Yield Asymmetry of Extruded Mg-Sn-Zn Alloy Through Ca Addition *Journal of Alloys and Compounds* 2018: pp. 1076–1086.  
<https://doi.org/10.1016/j.jallcom.2018.12.109>
10. **Jihua, C., Zhenhua, C., Hongge, Y., Fuquan, Z., Yingliang, C.** Effects of Sn and Ca Additions on Microstructure, Mechanical Properties, and Corrosion Resistance of the As-cast Mg-Zn-Al Based Alloy *Journal of Materials and Corrosion* 59 (12) 2008: pp. xx–xx.  
<https://doi.org/10.1002/maco.200805010>
11. **Liu, J., Bian, D., Zheng, Y., Chu, X., Lin, Y., Wang, M., Lin, Z., Li, M., Zhang, Y., Guan, S.** Comparative in Vitro Study on Binary Mg-RE (Sc, Y, La, Ce, Pr, Nd, Sm, Eu, Gd, Tb, Dy, Ho, Er, Tm, Yb and Lu) Alloy Systems *Journal of Acta BioMaterialia* S1742-7061 2019: pp. 30753–30756.  
<https://doi.org/10.1016/j.actbio.2019.11.013>
12. **Wang, Y.X., Fu, J.W., Yang, Y.S.** Effect of Nd Addition on Microstructures and Mechanical Properties of AZ80 Magnesium Alloys *Transactions of Nonferrous Metals Society of China* 22 (6) 2012: pp. 1322.  
[https://doi.org/10.1016/S1003-326\(11\)61321-6](https://doi.org/10.1016/S1003-326(11)61321-6)
13. **Xue, H., Yang, G., Li, D., Xing, Z., Pan, F.** Effects of Yttrium Addition on Microstructure and Mechanical Properties of AZ80–2Sn Magnesium Alloys *Journal of High Temperature Materials and Process* 34 (8) 2015: pp. 743–749.  
<https://doi.org/10.1515/htmp-2014-0095>
14. **Jiang, N., Chen, L., Meng, L., Fang, C., Hao, H., Zhang, X.** Effect of Neodymium, Gadolinium Addition on Microstructure and Mechanical Properties of AZ80 Magnesium Alloy *Journal of Rare Earths* 34 (6) 2016: pp. 632.  
[https://doi.org/10.1016/S1002-0721\(16\)60072-8](https://doi.org/10.1016/S1002-0721(16)60072-8)
15. **Yang, Z., Dingfei, Z., Renjie, L., Peng, W., Jingkai, F., Xia, C., Jiang, B., Pan, F.** Effect of Gd Addition on the Microstructure and Age Hardening Behaviour of Mg-6Zn-1Mn-4Sn Alloy *Journal of Materials Research and Technology* 9 (6) 2020: pp. 12737–12746.  
<https://doi.org/10.1016/j.jmrt.2020.09.010>
16. **Mishra, R.K., Gupta, A.K., Rao, P.R., Sachdev, A.K., Kumar, A.M., Luo, A.** Influence of Cerium on the Texture and Ductility of Magnesium Extrusions *Scripta Materialia* 59 2008: pp. 562–565.  
[https://doi.org/10.1007/978-3-319-48099-2\\_58](https://doi.org/10.1007/978-3-319-48099-2_58)
17. **Yu, H., Kim, Y.M., You, B.S., Yu, H.S., Park, S.H.** Effects of Cerium Addition on the Microstructure, Mechanical Properties and Hot Workability of ZK60 Alloy *Journal of Materials Science and Engineering A* 559 2013: pp. 798–807.  
<https://doi.org/10.1016/j.msea.2012.09.026>
18. **Che, Ch., Cai, Z., Yang, X., Cheng, L., Du, Y.** The Effect of Co-addition of Si, Ca and RE on Microstructure and Tensile Properties of As-extruded AZ91 Alloy *Journal of Materials science and Engineering A* 705 2017: pp. 282–290.  
<https://dx.doi.org/10.1016/j.msea.2017.08.026>
19. **Yang, M., Zhu, Y., Pan, F., Yang, H.** Effects of Minor Sr, Sn and Sc Addition on As-cast Microstructure and Mechanical Properties of ZA84 Magnesium Alloy *Transactions of Nonferrous Metals Society of China* 20 2010: pp. s306–s310.
20. **Jayalakshmi, S., Sankaranarayanan, S., Koh, S., Gupta, M.** Effect of Ag and Cu Trace Additions on the Micro Structural Evolution and Mechanical Properties of Mg–5Sn Alloy *Journal of Alloys and Compounds* 565 2013: pp.56–65.  
<https://dx.doi.org/10.1016/j.jallcom.2013.02.186>
21. **Pan, F., Yang, M.** Preliminary Investigations About Effects of Zr, Sc and Ce Additions on As-cast Microstructure and Mechanical Properties of Mg–3Sn–1Mn Magnesium Alloy *Journal of Materials Science and Engineering A* 528 2011: pp. 4973–4981.  
<https://dx.doi.org/10.1016/j.msea.2011.02.095>
22. **Pourbahari, B., Emamy, M., Mirzadeh, H.** Synergistic Effect of Al and Gd on Enhancement of Mechanical Properties of Magnesium Alloys *Journal of Progress in Natural Science: Materials International* 27 2017: pp. 228–235.  
<http://dx.doi.org/10.1016/j.pnsc.2017.02.004>
23. **Yang, Z., Xiao, Y.C., Ya-Lin, L., Xiao, P.L.** Microstructure and Mechanical Properties of As-extruded Mg-Sn-Zn-Ca Alloy with Different Extrusion Ratios *Transactions of Nonferrous Metals Society of China* 28 2018: pp. 2190–2198.  
[https://doi.org/10.1016/S1003-6326\(18\)64864-2](https://doi.org/10.1016/S1003-6326(18)64864-2)

